Int. J. Heat Mass Transfer. Vol. 17, pp. 915–931. Pergamon Press 1974. Printed in Great Britain

RADIATION–CONVECTION INTERACTION FOR A LATERALLY BOUNDED FLOW PAST A HOT PLATE

WERNER KOCH*
DFVLR-Institut für Theoretische Gasdynamik, Aachen, Federal Republic of Germany

(*Received* 2 *March* 1973)

Abstract—Radiation–convection interaction for a laterally bounded flow past a heated plate is investigated, whereby the influence of two-dimensional radiation is emphasized. Due to the high anisotropy of the radiation near the leading edge of the plate the ordinary, two-dimensional differential approximation fails in the vicinity of the edge. Therefore Olfe's modified differential approximation, which separately accounts for the external wall radiation, is employed. The equations for a gray gas are linearized under the assumption of small temperature perturbations and are solved by means of the Wiener–Hopf technique. The results are compared with several approximate solutions. Among other results it is shown that the one-dimensional "radiation-layer" model of Cess is limited to weak radiation. For intermediate and strong radiation a distinct precursor is observed.

NOMENCLATURE

A, $\frac{3}{2}a/(2-a)$;
$\mathscr{A}_n^{(0)}$, coefficient defined by (D.2);
$\mathscr{A}_{n,j}^{(1)}$, coefficient defined by (D.5);
a, total hemispherical absorptivity for a gray surface;
$\mathscr{B}_n^{(0)}$, coefficient defined by (A.9);
$\mathscr{B}_n^{(1)}$, coefficient defined by (D.6);
Bo, Boltzmann number, $Bo = \rho_\infty^* c_{p\infty}^* U_\infty^*/(\sigma^* T_\infty^{*3})$;
Bu, Bouguer number, $Bu = \alpha_\infty^* h^*$;
C_1, C_2, C_3, C_4, constants of integration;
$\mathscr{C}_n^{(1)}, \mathscr{C}_{n,j}^{(2)}$, coefficients defined by (28);
c_p^*, specific heat at constant pressure;
$D(\lambda)$, function defined by (24);
$\mathscr{D}_{n,j}^{(1)}, \mathscr{D}_n^{(2)}$, coefficients defined by (29);
$E_n(z)$, exponential integral function of order n;
$G(\lambda)$, function defined by (26);
h^*, semi-width of channel;
I, nondimensional, frequency-integrated perturbation intensity,

$$I = \frac{\pi(I^* - \sigma^* T_\infty^{*4}/\pi)}{4\sigma^* T_\infty^{*3}(T_p^* - T_\infty^*)};$$

Im, imaginary part of a (complex) function;
i, unit on imaginary axis;
$K(\lambda)$, kernel function defined by (15);
$Ki_n(z)$, nth repeated integral of the modified Bessel function $K_0(z)$, defined in Appendix C;
l, unit vector in ray direction;
M_n, coefficient defined by (21c);
$m(\lambda)$, function defined by (9);
$N_{n,j}$, coefficient defined by (D.4);
$Q(x, y)$, heat-source term defined in Appendix C;
q^R, dimensionless net radiative heat flux, $q^R = q^{*R}/\{4\sigma^* T_\infty^{*3}(T_P^* - T_\infty^*)\}$;
Re, real part of a (complex) function;
S_n, coefficient defined by (D.3);
s, propagation direction of I^*;
T^*, absolute temperature;
$T_{n,j}$, coefficient defined by (20a, b);
U_∞^*, free stream velocity parallel to plate;
u, v, functions defined by (13a, b);
x, y, nondimensional coordinates parallel and perpendicular to plate respectively, $x = x^*/h^*$, $y = y^*/h^*$.

Superscripts

$*$, dimensional quantity;
$\bar{}$, Fourier transformed quantity;
$\tilde{}$, modified zeros and poles as defined in Appendix B;
$\hat{}$, value according to one-dimensional model.

Subscripts

P, value on the plate;
∞, free stream value;
ext, quantity due to external wall radiation;
g, quantity due to gas emission;
W, value on the side walls;
$\oplus, \ominus$, functions of λ regular in an upper and lower half plane respectively.

---

*Present address: DFVLR/AVA—Abt. Theoret. Gasdynamik, D-34 Göttingen, Bunsenstr. 10, Germany.

Greek symbols

- α^*, volumetric absorption coefficient;
- $\pm\beta_n$, imaginary parts of the poles of K in the m-plane as defined in Appendix B;
- Γ, dimensionless radiation–convection parameter, $\Gamma = 16\,Bu/\{3\,Bo(1+Bu^2)\}$;
- $\pm\gamma_n$, imaginary parts of the zeros of K in the m-plane as defined in Appendix B;
- Δ, Laplace operator;
- ζ, η, dummy variables of integration;
- Θ, dimensionless temperature, $\Theta = (T^* - T^*_\infty)/(T^*_P - T^*_\infty)$;
- λ, Fourier transformation variable;
- $-\mu_k, \nu^{(j)}_k$, imaginary parts of the zeros of K as defined in Appendix B;
- ξ, dimensionless axial coordinate,

$$\xi = \frac{2\sigma^*\alpha^*_\infty T^{*3}_\infty x^*}{\rho^*_\infty c^*_{p\infty} U^*_\infty} \equiv 2\,Bu\,.\,x/Bo;$$

- Ω, solid angle;
- ρ^*, density;
- σ^*, Stefan–Boltzmann constant;
- $-\sigma_k, \tau^{(j)}_k$, imaginary parts of the poles of K as defined in Appendix B.

INTRODUCTION

THE TEMPERATURE field in a laminar flow past a flat plate at zero incidence is governed by the energy equation together with the conservation equations of mass and momentum. For a radiation absorbing and emitting medium, especially at higher temperatures, radiation phenomena become important and the equations of motion have to be modified to include electromagnetic radiation. While for vehicles flying at extreme velocities the cold-wall case with dissipative and shock heating is the one of interest, attention is focused in the present paper on investigating the radiative transfer induced by an isothermal hot plate. Such a problem has also possible application in the related fields of radiative heat transfer to a medium with suspended solid particles or in neutron transport theory.

For most engineering purposes the radiant energy density and the radiation stresses are negligible so that only the radiant heat-flux term in the energy equation provides a coupling with the radiation field. This results in a set of non-linear integro-differential equations and the difficulty of solving these for the title problem forces us to make drastic simplifications. First we limit ourselves to flows at high Reynolds and Péclét numbers, an assumption basic to most applications with convective–conductive heat transfer only. Then in many situations involving radiating media dissipative effects will still be confined to a relatively thin boundary layer near the plate and a singular perturbation technique similar to higher order boundary-layer theory can be used to find a solution.* Such a "weak interaction" model has been advanced successfully by Cess (see for example [2]), although he as well as most other investigators neglect the change of radiation in the direction parallel to the plate, thus defining a "radiation layer" outside the dissipative boundary layer. But compared to the effects of viscosity and heat-conduction radiation is in general a long-range phenomenon so that two-dimensional effects and hence precursor heating of the medium may be of importance in many physical situations. It is the objective of this investigation to elucidate this question. Therefore we are solving for what Cess calls the "outer region" where dissipative effects can be neglected, but we do keep the two-dimensional character of the radiation field. This way we find the first-order influence of convection upon radiation and vice-versa but are not concerned about radiation-conduction interaction which calls for a solution of the "inner region".

As noted by Vincenti and Traugott [3] such a two-dimensional treatment becomes manageable only with the help of linearization and the use of the differential approximation. But the differential approximation, being the lowest level in the spherical harmonics expansion, will be a good approximation only if the variation in the directional distribution of the intensity is sufficiently smooth. Unfortunately this is not the case for our problem where the intensity has a strongly non-isotropic character a few photon mean-free paths within the leading edge of the plate. Hence large errors of the ordinary differential approximation are to be expected there.

Based on the assumption that the failure of the usual differential approximation is due to radiation from the walls Olfe [4] devised a conceptually very simple modified differential approximation.† We hasten to add that this modified differential approximation, although very simple in concept, may prove prohibitively difficult in an actual problem with more complicated boundaries. Morevoer, recent investigations [7, 8, 9], also aimed at improving the differential approximation, indicate severe limitations of Olfe's modification in the case of cold walls or internal heat

*As in higher order boundary-layer theory the solution will not be uniformly valid far downstream. Mathematically second-order effects eventually become of first-order, i.e. in our case with growing boundary-layer thickness the boundary layer cannot be considered optically thin any more, thus leading to the solution of Viskanta and Grosh [1] for optically thick boundary layers.

†Similar modifications have been published by Landram and Greif [5] and Glicksman [6].

generation. Nevertheless, this modified differential approximation seems to be applicable in the case of our problem and since good results were obtained for the one-dimensional test case published previously [10], Olfe's method will also be employed in the present investigation. Keeping in mind the fact that no exact solution of the two-dimensional problem exists, it is hoped that the results obtained by means of the modified differential approximation not only give a good qualitative picture but are also fairly good quantitatively.

FORMULATION OF THE PROBLEM

While Olfe's modification approximately takes care of the failure of the ordinary differential approximation near the leading edge in our problem we still have to face the spectral difficulty. The simplest but for most media rather unrealistic simplification is the assumption of a gray gas. For our exploratory purposes, where we try to find the basic influence of the radiation–convection parameter Γ, the notion of a gray gas with a volumetric absorption coefficient α^* is good enough as a first model but we shall return to this question briefly at the end of the paper. In addition to neglecting the frequency dependence we assume the medium to be non-scattering and of unit index of refraction, whereas all bounding walls are taken to be black for simplicity and also to display the maximum wall influence. For only small deviations from radiative equilibrium, i.e. $(T_P^* - T_\infty^*)/T_\infty^* \ll 1$, we may linearize and, omitting heat conduction and viscous effects, we obtain for the energy equation in terms of our non-dimensional quantities defined in the Nomenclature

$$Bo\frac{\partial \Theta}{\partial x} + 4\,\mathrm{div}\,\boldsymbol{q}^R = 0. \tag{1}$$

Here the Boltzmann number Bo gives the ratio of the free stream convective energy flux to the black-body radiative flux at free stream temperature.

According to Olfe's modified differential approximation the net radiative flux $\boldsymbol{q}^R$ at each point is split into two parts

$$\boldsymbol{q}^R = \boldsymbol{q}_g + \boldsymbol{q}_{\mathrm{ext}}, \tag{2}$$

where $\boldsymbol{q}_{\mathrm{ext}}$ is the flux contributed by the non-isotropic external wall radiation (to be computed in Appendix C), while $\boldsymbol{q}_g$ is the flux contributed by gas emission. The latter can be adequately described by means of the differential approximation (see for example [11, 12])

$$\mathrm{div}\,\boldsymbol{q}_g = 4\,Bu(\Theta - I_g), \tag{3}$$

$$\mathrm{grad}\,I_g = -\tfrac{3}{4}Bu\,\boldsymbol{q}_g. \tag{4}$$

Bu denotes the Bouguer number formed with a characteristic length h^* to be introduced below. Equations (1), (3) and (4) can now be combined and in our case it is advantageous to formulate the problem in terms of the intensity I_g:

$$\frac{Bo}{3\,Bu^2}\Delta\left(\frac{\partial I_g}{\partial x} + \frac{16\,Bu}{Bo}I_g\right) - Bo\frac{\partial I_g}{\partial x} = Q(x, y). \tag{5}$$

The distribution of heat sources $Q(x, y) \equiv 4\,\mathrm{div}\,\boldsymbol{q}_{\mathrm{ext}}$ introduced by the wall radiation is evaluated in Appendix C. For zero convection $Bo = 0$ and the above equation reduces to a Poisson equation.

To complete the formulation of our boundary-value problem we have to prescribe the pertinent boundary conditions. The problem of most interest is the flow past a finite or semi-infinite hot plate in an otherwise unbounded stream. Since equation (5) is linear and admits a separation of variables solution the boundary-value problem could be solved by superposition such that the upstream and downstream solution match along the line $x = 0$ at the leading edge of the plate. At the same time the boundary condition on the plate has to be satisfied. This is not an easy task. On the other hand this mixed boundary-value problem is a typical example for the application of the Wiener–Hopf technique. But here the difficulty shows up in the factoring of a complex function with three branch cuts. This difficulty forced us to solve first a simpler problem where only poles but no branch cuts are involved, or in other words a problem whose solution can be expressed in terms of a Fourier series rather than a Fourier integral. There are several ways of accomplishing this. We have chosen the problem depicted in Fig. 1 where a semi-infinite opaque plate of temperature T_P^* is located symmetrically between two parallel walls of free-stream temperature $T_\infty^* < T_P^*$ and moving with U_∞^*. This laterally bounded problem also allows us to study the precursor effect and furthermore has the advantage that far downstream it's solution approaches the well-documented one-dimensional case of radiative transfer in an emitting–absorbing medium

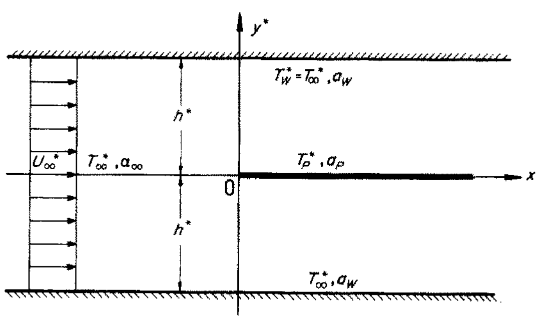

FIG. 1. Geometry of the problem.

between two walls. The disadvantage is that by introducing the channel half-width h^* as a definite geometrical length an additional parameter, namely Bu, has to be accounted for.

Due to the symmetry of the problem we only need to solve for $y \geq 0$. Since the net flux q_g in y-direction is zero along $y = 0$, $x < 0$, equation (4) gives us the condition

$$\frac{\partial I_g}{\partial y}(x, 0) = 0 \quad \text{for} \quad x < 0. \tag{6}$$

The boundary condition for I_g on the remaining boundary can be determined within the framework of the differential approximation and is written in the form (see for example [12])

$$\frac{\partial I_g}{\partial y}(x, 1) + A_W Bu I_g(x, 1) = 0, \tag{7}$$

and for $x > 0$

$$\frac{\partial I_g}{\partial y}(x, 0^+) - A_P Bu I_g(x, 0^+) = \begin{cases} -A_P Bu & \text{(8a)} \\ 0 & \text{(8b)} \end{cases}.$$

The constant A is defined in the Nomenclature and, for our assumed black-body walls, takes the value

$$A_W = A_P = A = 3/2.$$

The inhomogeneous boundary condition (8a) is relevant for the ordinary differential approximation. In Olfe's modified differential approximation the radiation from the plate is taken care of by q_{ext} and hence the homogeneous boundary condition (8b) applies in this case.

We proceed now by first solving the problem by means of the much simpler ordinary differential approximation. Not only are large portions of the analysis common to both methods but it is also quite instructive to compare the two results.

SOLUTION ACCORDING TO THE ORDINARY DIFFERENTIAL APPROXIMATION

As mentioned before the above formulated problem is a typical example of the application of the Wiener–Hopf technique in conjunction with the two-sided Fourier transform defined by

$$\bar{f}(\lambda) = \int_{-\infty}^{\infty} e^{-i\lambda x} f(x)\, dx,$$

with the inverse transformation

$$f(x) = \frac{1}{2\pi} \int_{-\infty}^{\infty} e^{i\lambda x} \bar{f}(\lambda)\, d\lambda.$$

Thus taking the Fourier transform of the homogeneous equation (5) with respect to x we find

$$\frac{d^2 \bar{I}_g}{dy^2} - m^2 \bar{I}_g = 0,$$

$$m(\lambda) = \{\lambda(\lambda^2 + 3Bu^2 - i\lambda 16 Bu/Bo)/(\lambda - i16 Bu/Bo)\}^{1/2} \tag{9}$$

with the general solution

$$\bar{I}_g(y; \lambda) = C_1(\lambda) e^{my} + C_2(\lambda) e^{-my}. \tag{10}$$

Similarly, after taking the Fourier transform, we can write the boundary conditions (6), (7) and (8a) in the form

$$\frac{d\bar{I}_g}{dy}(1; \lambda) + \tfrac{3}{2} Bu \bar{I}_g(1; \lambda) = 0, \tag{11}$$

$$\bar{I}_g(0; \lambda) = \bar{u}(\lambda)_\oplus - i/\lambda + \frac{2}{3\, Bu} \bar{v}(\lambda)_\ominus. \tag{12}$$

Here $\bar{u}_\oplus$ and $\bar{v}_\ominus$ are the Fourier transforms of the functions

$$u(x) = \begin{cases} I_g(x, 0), & x < 0 \\ 0, & x < 0 \end{cases} \tag{13a}$$

$$v(x) = \begin{cases} 0, & x < 0 \\ \dfrac{\partial I_g}{\partial y}(x, 0^+), & x > 0 \end{cases} \tag{13b}$$

which are unknown on complementary semi-infinite lines. $\bar{u}_\oplus$ and $\bar{v}_\ominus$ are regular functions of λ in an upper and lower half plane denoted by the subscript $\oplus$ and $\ominus$ respectively. The *a priori* assumption that these half planes overlap is standard but has to be checked once the result has been found.

Now, using (11), (12) and the Fourier transformed definition (13b), we express the constants C_1 and C_2 of the general solution (10) in terms of $\bar{u}_\oplus$ and $\bar{v}_\ominus$ and end up with the governing Wiener–Hopf equation

$$\bar{u}(\lambda)_\oplus - \bar{v}(\lambda)_\ominus / K(\lambda) = i/\lambda, \tag{14}$$

which is valid in the strip of regularity $-\mu_1 < Im\lambda < 0$. In writing $-i/\lambda$ in (12) as the Fourier transform of Heaviside's unit function we have already assumed $Im\lambda < 0$ while the asymptotic behavior $I_g \sim \exp(\mu_1 x)$ for $x \to -\infty$ gives the lower limit of the upper half plane. Also it is easy to prove that

$$K(\lambda) = \frac{-\left(\cosh m + \dfrac{2m}{3\, Bu} \sinh m\right)}{\dfrac{4}{3\, Bu} \cosh m + \dfrac{\sinh m}{m}\left[1 + \left(\dfrac{2m}{3\, Bu}\right)^2\right]} \tag{15}$$

is a single-valued function of λ. Besides the point at infinity, both numerator and denominator of K have another accumulation point of simple zeros at

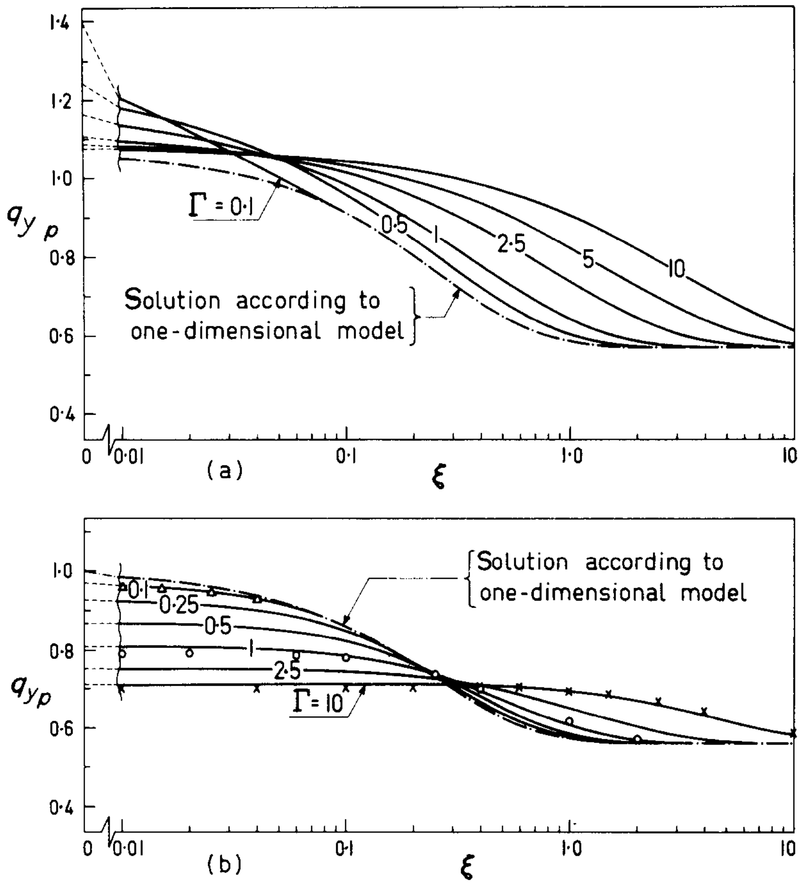

FIG. 2. Two-dimensional solution for the non-dimensional linearized radiative heat flux normal to the black-body plate as a function of ξ and Γ for $Bu = 1$. (a) Solution according to the ordinary differential approximation. (b) Solution according to Olfe's modified differential approximation with one-dimensional (solid lines) and two-dimensional (marked points) external wall radiation.

$\lambda = i16Bu/Bo$. Nevertheless Weierstrass' infinite-product theorem can still be applied to factor K into two regular and zeroless functions of algebraic growth as $\lambda \to \infty$ in the appropriate half plane, i.e.

$$K = K_{\oplus} K_{\ominus} \tag{16}$$

where

$$K(\lambda; Bu, \Gamma)_{\oplus} = -\frac{3\,Bu/2}{2+3\,Bu/2} \prod_{k=1}^{\infty} \frac{\{1+\lambda/(i\mu_k)\}}{\{1+\lambda/(i\sigma_k)\}} \tag{17a}$$

$$K(\lambda; Bu, \Gamma)_{\ominus} = \prod_{j=1}^{2} \prod_{k=1}^{\infty} \frac{\{1-\lambda/(i\nu_k^{(j)})\}}{\{1-\lambda/(i\tau_k^{(j)})\}}. \tag{17b}$$

Here we introduced, instead of Bo, the dimensionless radiation–convection parameter

$$\Gamma = 16\,Bu/\{3\,Bo(1+Bu^2)\}$$

which measures the ratio of radiative to convective energy transport (compare [12], p. 103). The explicit values of the zeros $-i\mu_k$, $i\nu_k^{(j)}$ and poles $-i\sigma_k$, $i\tau_k^{(j)}$, $j = 1, 2;\ k = 1, 2, \ldots,$ are given in Appendix B. The Wiener–Hopf equation (14) is now solved in the usual manner (cf. Noble [13]). Separation into two parts regular in an upper and lower half plane respectively defines an integral function of λ which is taken to be identically zero to yield the least singular solution. Thus

$$\bar{v}(\lambda)_{\ominus} = i\frac{3\,Bu/2}{2+3\,Bu/2} K(\lambda)_{\ominus}/\lambda, \tag{18}$$

$$\bar{u}(\lambda)_{\oplus} = \frac{i}{\lambda}\left[1 + \frac{3\,Bu/2}{2+3\,Bu/2}\Big/ K(\lambda)_{\oplus}\right].$$

Taking into account equation (4) the inversion of (18) by means of the residue theorem* gives at once the

*The inversion contour has to be deformed such that the accumulation points of poles at infinity and at $\lambda = i16\,Bu/Bo$ are circumvened properly.

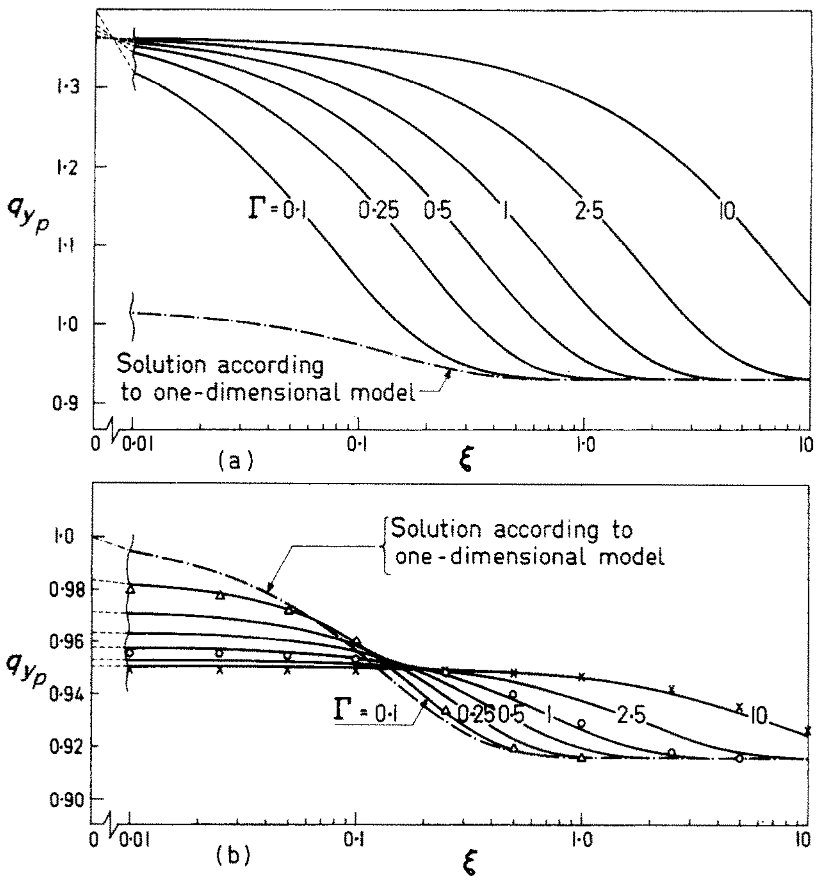

FIG. 3. Two-dimensional solution for the non-dimensional linearized radiative heat flux normal to the black-body plate as a function of ξ and Γ for $Bu = 0{\cdot}1$. (a) Solution according to the ordinary differential approximation. (b) Solution according to Olfe's modified differential approximation with one-dimensional (solid lines) and two-dimensional (marked points) external wall radiation.

heat flux normal to the plate. In terms of the "radiation-layer" variable ξ, introduced by Cess [2], we obtain for $\xi \geqslant 0$

$$q_y^R(\xi, 0^+) = \frac{1}{1+3\,Bu/4} \times \left\{1 - \sum_{j=1}^{2} \sum_{n=1}^{\infty} T_{n,j} \exp(-\tilde{\tau}_n^{(j)}\xi)\right\}, \quad (19)$$

$$T_{n,1} = \frac{(1-\tilde{\tau}_n^{(1)}/\tilde{\nu}_n^{(1)})(1-\tilde{\tau}_n^{(1)}/\tilde{\nu}_n^{(2)})}{(1-\tilde{\tau}_n^{(1)}/\tilde{\tau}_n^{(2)})} \times \prod_{k(\neq n)=1}^{\infty} \frac{(1-\tilde{\tau}_n^{(1)}/\tilde{\nu}_k^{(1)})(1-\tilde{\tau}_n^{(1)}/\tilde{\nu}_k^{(2)})}{(1-\tilde{\tau}_n^{(1)}/\tilde{\tau}_k^{(1)})(1-\tilde{\tau}_n^{(1)}/\tilde{\tau}_k^{(2)})} \quad (20a)$$

$$T_{n,2} = \frac{(1-\tilde{\tau}_n^{(2)}/\tilde{\nu}_n^{(1)})(1-\tilde{\tau}_n^{(2)}/\tilde{\nu}_n^{(2)})}{(1-\tilde{\tau}_n^{(2)}/\tilde{\tau}_n^{(1)})} \times \prod_{k(\neq n)=1}^{\infty} \frac{(1-\tilde{\tau}_n^{(2)}/\tilde{\nu}_k^{(1)})(1-\tilde{\tau}_n^{(2)}/\tilde{\nu}_k^{(2)})}{(1-\tilde{\tau}_n^{(2)}/\tilde{\tau}_k^{(1)})(1-\tilde{\tau}_n^{(2)}/\tilde{\tau}_k^{(2)})}. \quad (20b)$$

Numerical results for the radiative heat flux q_y^R normal to the plate are shown in Figs. 2a and 3a for $Bu = 1$ and $Bu = 0{\cdot}1$ respectively as well as for several values of Γ. Since in our problem the radiative heat flux cannot be larger than for a fully transparent gas the results are clearly erroneous near the leading edge due to the failure of the ordinary differential approximation.

In particular the heat flux is too high there, a tendency that, although less pronounced, already shows up in the one-dimensional solution (compare Fig. 5). For comparison the result according to this one-dimensional "radiation layer" model is indicated by the dotted curve.

The general solution (10) for $\bar{I}_g$ in the complex plane with C_1 and C_2 expressed in terms of $\bar{v}_\ominus$ and $\bar{u}_\oplus$ is given by

$$\bar{I}(y;\lambda)_g = \frac{m\cosh[m(1-y)] + (3\,Bu/2)\sinh[m(1-y)]}{m\cosh m + (3\,Bu/2)\sinh m} \times \left\{\bar{u}_\oplus + \frac{2}{3\,Bu}\bar{v}_\ominus - i/\lambda\right\}.$$

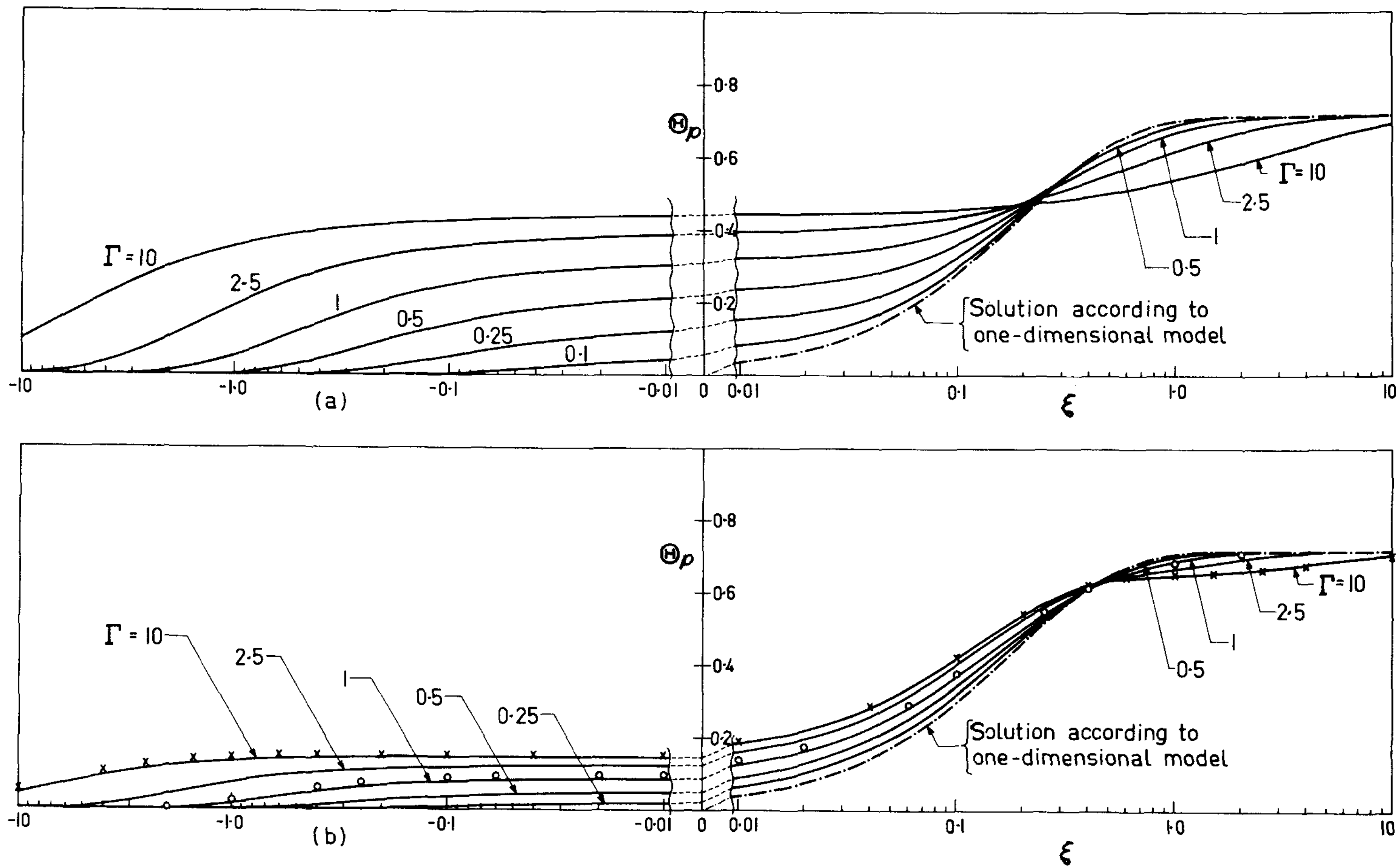

FIG. 4. Two-dimensional solution for the non-dimensional gas temperature on $y = 0$ as a function of ξ and Γ for $Bu = 1$. (a) Solution according to the ordinary differential approximation. (b) Solution according to Olfe's modified differential approximation with one-dimensional (solid lines) and two-dimensional (marked points) external wall radiation.

Once $\bar{I}_g$ is determined, the temperature $\bar{\Theta}$ in the complex plane can be evaluated in terms of $\bar{I}_g$ by combining the transformed equations (1) and (3), namely

$$\bar{\Theta}(y;\lambda) = -\frac{i16\,Bu/Bo}{\lambda - i16\,Bu/Bo}\,\bar{I}(y;\lambda)_g.$$

Inversion of $\bar{I}_g$ and $\bar{\Theta}$ by means of the residue theorem then gives the final results in Fourier-series form. For $\xi \leqslant 0$ and $0 \leqslant y \leqslant 1$ we obtain

$$\begin{Bmatrix} I(\xi,y)_g \\ \Theta(\xi,y) \end{Bmatrix} = \sum_{n=1}^{\infty} \begin{Bmatrix} 1 \\ 8/(8+\tilde{\mu}_n) \end{Bmatrix} M_n \times \exp(\tilde{\mu}_n \xi)\cos(\gamma_n y), \quad (21\text{a, b})$$

$$M_n = (1-\tilde{\mu}_n/\tilde{\sigma}_n)\prod_{k(\neq n)=1}^{\infty}\frac{(1-\tilde{\mu}_n/\tilde{\sigma}_k)}{(1-\tilde{\mu}_n/\tilde{\mu}_k)}. \quad (21\text{c})$$

Similarly, for $\xi \geqslant 0$ and $0 \leqslant y \leqslant 1$

$$\begin{Bmatrix} I(\xi,y)_g \\ \Theta(\xi,y) \end{Bmatrix} = \frac{1}{2+3\,Bu/2}\Bigg[1 + 3\,Bu(1-y)/2 + \sum_{j=1}^{2}\sum_{n=1}^{\infty}\begin{Bmatrix} 1 \\ 8/(8-\tilde{\tau}_n^{(j)}) \end{Bmatrix} T_{n,j}\exp(-\tilde{\tau}_n^{(j)}\xi) \times \left\{\cos(\beta_n y) + \frac{3\,Bu}{2\beta_n}\sin(\beta_n y)\right\}\Bigg]. \quad (22\text{a, b})$$

Here γ_n and β_n, as defined in Appendix B, are the absolute values of the imaginary zeros and poles of K in the m-plane respectively. It can be checked immediately that for $\xi \to \infty$ both the two-dimensional results (19) and (21) as well as the one-dimensional results (A.7) and (A.8) approach the well-studied solution for a radiatively participating medium between two infinite walls according to the differential approximation. Numerical results for the gas temperature Θ at $y = 0$ are shown in Fig. 4(a) for the specific case $Bu = 1$. The indicated asymptotic results at $\xi = 0$ are obtained in the usual fashion by letting $\lambda \to \infty$ in the appropriate complex half plane before inverting. Due to the failure of the ordinary differential approximation near the leading edge these results are expected to be in error for small ξ.

SOLUTION ACCORDING TO OLFE'S MODIFIED DIFFERENTIAL APPROXIMATION

As before the Wiener–Hopf technique may be used in solving the now inhomogeneous equation (5) together with the homogeneous boundary conditions (6), (7) and (8b). The standard procedure (see [13], p. 87) employs the method of superposition, but we may also perform the additive decomposition directly.* We take the Fourier transform of (5) noting that the appropriate domain in the λ-plane will again be a strip below the real axis since $Q(x, y)$ behaves exponentially for $x \to -\infty$ and approaches a constant as $x \to +\infty$. Thus we find

$$\frac{\mathrm{d}^2\bar{I}_g}{\mathrm{d}y^2} - m^2\bar{I}_g = \frac{3\,Bu^2}{iBo}\,\frac{1}{\lambda - i16\,Bu/Bo}\,\bar{Q}(y;\lambda)$$

with the general solution

$$\bar{I}(y;\lambda)_g = C_3(\lambda)\,\mathrm{e}^{my} + C_4(\lambda)\,\mathrm{e}^{-my} + \bar{I}_{g_{\text{part}}}. \quad (23)$$

A particular solution $\bar{I}_{g_{\text{part}}}$ is easily found by the method of variation of parameters

$$\bar{I}_{g_{\text{part}}}(y;\lambda) = \frac{3}{2}\,\frac{Bu^2}{iBo}\,\frac{1}{m(\lambda - i16\,Bu/Bo)} \times \left\{\mathrm{e}^{my}\int_0^y \mathrm{e}^{-m\eta}\bar{Q}(\eta;\lambda)\,\mathrm{d}\eta - \mathrm{e}^{-my}\int_0^y \mathrm{e}^{m\eta}\bar{Q}(\eta;\lambda)\,\mathrm{d}\eta\right\}.$$

Now the procedure is equivalent to the one outlined in the previous section only, due to the homogeneous boundary condition (8b), the term i/λ has to be omitted in (12). Elimination of the constants of integration C_3 and C_4 in terms of $\bar{u}_\oplus$ and $\bar{v}_\ominus$ by means of the Fourier transformed boundary conditions yields the Wiener–Hopf equation

$$\bar{u}(\lambda)_\oplus - \bar{v}(\lambda)_\ominus/K(\lambda) = D(\lambda)/K(\lambda)_\oplus$$

valid in a strip below the real axis. Contrary to equation (14) the inhomogeneous term in the above Wiener–Hopf equation originates from the inhomogeneous term in the governing equation (5) and not from the boundary condition. We have

$$D(\lambda) = \frac{iK_\oplus 3\,Bu^2/Bo}{\lambda - i16\,Bu/Bo}\;\frac{\displaystyle\int_0^1\left\{\cosh[m(1-\eta)] + \frac{3\,Bu}{2m}\sinh[m(1-\eta)]\right\}\bar{Q}(\eta;\lambda)\,\mathrm{d}\eta}{\dfrac{3\,Bu}{2}\cosh m + m\sinh m}. \quad (24)$$

With the multiplicative factoring of K given by (16) and (17) we need to decompose $D(\lambda)$ additively into two parts regular in an upper and lower half plane. We write formally

$$D(\lambda) = D(\lambda)_\oplus + D(\lambda)_\ominus$$

and refer to Appendix D for the explicit decomposition.

*Equivalently we could also apply the Green's function method for a non self-adjoint boundary-value problem (see for example [14]). But the evaluation of Green's function in our particular case also leads to a Wiener–Hopf problem.

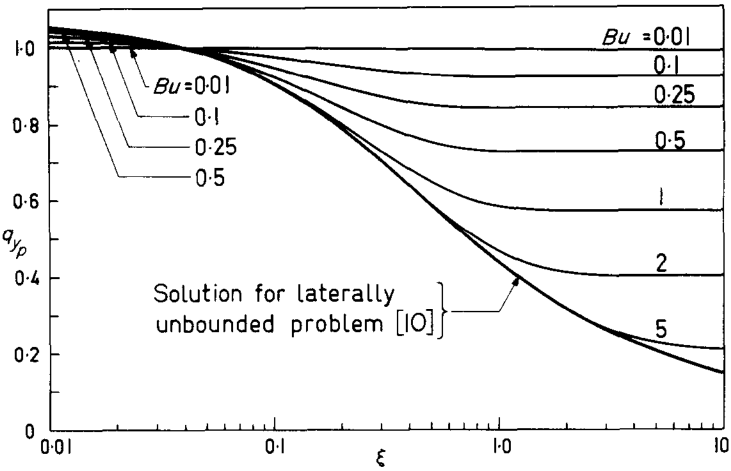

FIG. 5. One-dimensional solution for the non-dimensional linearized radiative heat flux normal to the black-body plate as a function of ξ and Bu according to the ordinary differential approximation.

Then separating the functions, regular in an upper and lower half plane, and again setting zero the integral function we obtain

$$\begin{aligned}\bar{u}(\lambda)_{\oplus} &= D(\lambda)_{\oplus}/K(\lambda)_{\oplus}\\ \bar{v}(\lambda)_{\ominus} &= -D(\lambda)_{\ominus}K(\lambda)_{\ominus}.\end{aligned} \tag{25}$$

With C_3 and C_4 of (23) expressed in terms of $\bar{u}_{\oplus}$ and $\bar{v}_{\ominus}$ we find our general solution I_g by inverting

$$\bar{I}(y;\lambda)_g = \frac{m\cosh[m(1-y)] + (3\,Bu/2)\sinh[m(1-y)]}{m\cosh m + (3\,Bu/2)\sinh m}\times\left\{\bar{u}_{\oplus} + \frac{2}{3\,Bu}\bar{v}_{\ominus} + G\right\} - \exp(my)G + \bar{I}_{g_{\text{part}}},$$

where we introduced the abbreviation

$$G(\lambda) = -\frac{\exp(-m)}{m+3\,Bu/2}\times\{(3\,Bu/2)\cosh m + m\sinh m\}D(\lambda)/K(\lambda)_{\oplus}. \tag{26}$$

Once again $\bar{\Theta}$ can be expressed in terms of $\bar{I}_g$ by combining the Fourier transformed equations (1), (2) and (3) together with the definition (C.1) such that

$$\bar{\Theta}(y;\lambda) = -\frac{i16\,Bu/Bo}{\lambda - i16\,Bu/Bo}\bar{I}(y;\lambda)_g + \frac{i}{Bo}\frac{\bar{Q}(y;\lambda)}{\lambda - i16\,Bu/Bo}. \tag{27}$$

In principle all quantities can now be evaluated at any point but for simplicity we concentrate on computing the gas temperature and the heat flux normal to the plate, both at $y = 0$. For the latter we basically need the inversion of (25), while $\Theta(x, 0)$ can be obtained by setting $y = 0$ in (27) and inverting. The inversion integrals are evaluated by means of the residue theorem resulting in a rather lengthy series representation. For $\xi \leqslant 0$ we obtain

$$\Theta(\xi,0) = \sum_{n=1}^{\infty}\frac{8M_n\exp(\tilde{\mu}_n\xi)}{8+\tilde{\mu}_n}\left\{\sum_{m=1}^{\infty}\frac{S_m(8\,Bu\,\mathscr{B}_m^{(0)} - \sigma_m\mathscr{B}_m^{(1)})}{(8+\tilde{\sigma}_m)(1-\tilde{\sigma}_m/\tilde{\mu}_n)} + 2(1+3\,Bu/4)\sum_{j=1}^{2}\sum_{m=1}^{\infty}\frac{v_m^{(j)}N_{m,j}\mathscr{A}_{m,j}^{(1)}}{(\tilde{v}_m^{(j)}-8)(1+\tilde{v}_m^{(j)}/\tilde{\mu}_n)}\right\}$$
$$+16(1+3\,Bu/4)\left\{\sum_{n=1}^{\infty}\frac{\mu_nM_n\mathscr{C}(\xi)_n^{(1)}}{(8+\tilde{\mu}_n)^2}\prod_{k=1}^{\infty}\frac{(1+\tilde{\mu}_n/\tilde{\tau}_k^{(1)})(1+\tilde{\mu}_n/\tilde{\tau}_k^{(2)})}{(1+\tilde{\mu}_n/\tilde{v}_k^{(1)})(1+\tilde{\mu}_n/\tilde{v}_k^{(2)})} + \sum_{j=1}^{2}\sum_{n=1}^{\infty}\frac{v_n^{(j)}N_{n,j}\mathscr{C}(\xi)_{n,j}^{(2)}}{(\tilde{v}_n^{(j)}-8)^2}\prod_{k=1}^{\infty}\frac{(1+\tilde{v}_n^{(j)}/\tilde{\sigma}_k)}{(1+\tilde{v}_n^{(j)}/\tilde{\mu}_k)}\right\}.$$

Similarly for $\xi \geqslant 0$

$$\begin{Bmatrix}q_y^R(\xi,0^+)\\ \Theta(\xi,0)\end{Bmatrix} = \begin{Bmatrix}[1+E_3(Bu)-3E_4(Bu)/2]/(1+3\,Bu/4)\\ [1+3\,Bu/2-E_3(Bu)+3E_4(Bu)/2]/(2+3\,Bu/2)\end{Bmatrix}$$
$$+\sum_{j=1}^{2}\sum_{n=1}^{\infty}\begin{Bmatrix}1\\ 4/(\tilde{\tau}_n^{(j)}-8)\end{Bmatrix}T_{n,j}\exp(-\tilde{\tau}_n^{(j)}\xi)\Bigg[(3\,Bu/4 - E_3(Bu) + 3E_4(Bu)/2)/(1+3\,Bu/4)$$
$$+2\sum_{i=1}^{2}\sum_{m=1}^{\infty}\frac{N_{m,i}(8\,Bu\,\mathscr{A}_m^{(0)} - v_m^{(i)}\mathscr{A}_{m,i}^{(1)})}{(\tilde{v}_m^{(i)}-8)(1-\tilde{v}_m^{(i)}/\tilde{\tau}_n^{(j)})} + \frac{1}{1+3\,Bu/4}\sum_{m=1}^{\infty}\frac{\sigma_mS_m\mathscr{B}_m^{(1)}}{(8+\tilde{\sigma}_m)(1+\tilde{\sigma}_m/\tilde{\tau}_n^{(j)})}\Bigg]$$
$$+\frac{1}{1+3\,Bu/4}\sum_{j=1}^{2}\sum_{n=1}^{\infty}\begin{Bmatrix}1\\ 4/(\tilde{\tau}_n^{(j)}-8)\end{Bmatrix}\frac{\tau_n^{(j)}T_{n,j}\mathscr{D}(\xi)_{n,j}^{(1)}}{\tilde{\tau}_n^{(j)}-8}\prod_{k=1}^{\infty}\frac{(1+\tilde{\tau}_n^{(j)}/\tilde{\mu}_k)}{(1+\tilde{\tau}_n^{(j)}/\tilde{\sigma}_k)}$$
$$+\frac{1}{1+3\,Bu/4}\sum_{n=1}^{\infty}\begin{Bmatrix}-1\\ 4/(8+\tilde{\sigma}_n)\end{Bmatrix}\frac{\sigma_nS_n\mathscr{D}(\xi)_n^{(2)}}{8+\tilde{\sigma}_n}\prod_{k=1}^{\infty}\frac{(1+\tilde{\sigma}_n/\tilde{v}_k^{(1)})(1+\tilde{\sigma}_n/\tilde{v}_k^{(2)})}{(1+\tilde{\sigma}_n/\tilde{\tau}_k^{(1)})(1+\tilde{\sigma}_n/\tilde{\tau}_k^{(2)})}.$$

The coefficients $\mathscr{C}_n$ and $\mathscr{D}_n$ are defined by

$$\mathscr{C}(\xi)_n^{(1)} = \int_{\eta=0}^{1} \cos(\gamma_n \eta) \int_{\zeta=0}^{|\xi| Bo/(2Bu)} Q'(\zeta,\eta) \times \exp\{\tilde{\mu}_n(\xi + 2Bu\zeta/Bo)\}\, d\zeta\, d\eta, \quad (28a)$$

$$\mathscr{C}(\xi)_{n,j}^{(2)} = \int_{\eta=0}^{1} \cos(\gamma_n \eta) \int_{\zeta=|\xi| Bo/(2Bu)}^{\infty} Q'(\zeta,\eta) \times \exp\{-\tilde{v}_n^{(j)}(2Bu\zeta/Bo + \xi)\}\, d\zeta\, d\eta, \quad (28b)$$

$$\mathscr{D}(\xi)_{n,j}^{(1)} = \int_{\eta=0}^{1} \{\cos(\beta_n \eta) + \frac{3Bu}{2\beta_n}\sin(\beta_n \eta)\} \int_{\zeta=0}^{\xi Bo/(2Bu)} \times Q'(\zeta,\eta)\exp\{-\tilde{\tau}_n^{(j)}(\xi - 2Bu\zeta/Bo)\}\, d\zeta\, d\eta, \quad (29a)$$

$$\mathscr{D}(\xi)_n^{(2)} = \int_{\eta=0}^{1} \{\cos(\beta_n \eta) + \frac{3Bu}{2\beta_n}\sin(\beta_n \eta)\} \int_{\zeta=\xi Bo/(2Bu)}^{\infty} \times Q'(\zeta,\eta)\exp\{-\tilde{\sigma}_n(2Bu\zeta/Bo - \xi)\}\, d\zeta\, d\eta. \quad (29b)$$

Formulas as the ones listed above only make sense if general conclusions can be drawn from them and numerical results are given. First we note that, if only $\mathscr{A}_m^{(0)}$ and $\mathscr{B}_m^{(0)}$ are kept while the remaining coefficients $\mathscr{A}_m$, $\mathscr{B}_m$, $\mathscr{C}_m$ and $\mathscr{D}_m$ are all set identically zero, we have the solution for the two-dimensional equations but for a one-dimensional discontinuous heat-source distribution. Since $\mathscr{A}_m^{(0)}$ and $\mathscr{B}_m^{(0)}$ can be integrated explicitly the corresponding results for q^R and Θ are obtained comparatively easily and are depicted in Figs. 2b and 4b for $Bu = 1$ and in Fig. 3b for $Bu = 0{\cdot}1$. The results according to the exact two-dimensional source distribution at several points are indicated by triangles, circles and crosses for $\Gamma = 0{\cdot}1$, 1 and 10 respectively. It is clear that the temperature distribution due to the discontinuous source function has to have a discontinuous slope at $x = 0$ while the continuous two-dimensional source function smoothens this kink. The numerical procedure for obtaining the latter results is rather cumbersome but it is quite surprising how well the solution according to the one-dimensional source distribution approximates the fully two-dimensional results. This fact might prove useful in more complicated problems where the two-dimensional source distribution cannot be evaluated explicitly. For comparison the solution found by using the one-dimensional "radiation-layer" model is also given and marked by the dotted curve. As can be seen quite large deviations occur due to the two-dimensional character of the radiation field unless Γ is very small.

REMARKS ABOUT NON-GRAY GAS RADIATION

We conclude this section with a few remarks about the effects of non-gray gas radiation. An exact treatment is very difficult and differs for each medium but useful approximate results can be obtained by employing some of the several models proposed in the literature. For a "gray-band" model the changes in the differential approximation are outlined in [15]. According to [4] I_{ext} would then represent the integral of the wall spectral intensity over the width of the gas absorption band while the radiation outside of this band would not effect the state of the gas. Similarly Traugott's [16] modification of the differential approximation can be used if the frequency variation of the absorption coefficient is smooth enough. In this case the linear Planck mean absorption coefficient $\alpha_{LP\infty}^*$ as defined by Cogley *et al.* [17] has to be used for our linearized problem. In applying the ordinary differential approximation (i.e. $Q \equiv 0$) the governing equation (5) as well as the boundary conditions (6), (7) and (8a) and hence the solution remains the same if we redefine

$$Bu = h^*\{\alpha_{LP_\infty}^* \alpha_{R_\infty}^*\}^{1/2},$$

$$Bo = \rho_\infty^* c_{p_\infty}^* U_\infty^* (\alpha_{R_\infty}^*/\alpha_{LP_\infty}^*)^{1/2}/(\sigma^* T_\infty^{*3}),$$

$$A = \frac{3}{2}\frac{a}{2-a}(\alpha_{R_\infty}^*/\alpha_{LP_\infty}^*)^{1/2}.$$

Here $\alpha_{R_\infty}^*$ is the Rosseland mean free absorption coefficient evaluated at free stream conditions.

Accordingly Traugott's and Olfe's modification can be applied simultaneously. In this case we have to redefine

$$Q = 4(\alpha_{R_\infty}^*/\alpha_{LP_\infty}^*)^{1/2} \operatorname{div} \boldsymbol{q}_{ext}$$

and for the computation of $\boldsymbol{q}_{ext}$ again $\alpha_{LP_\infty}^*$ has to be used. But contrary to the analysis for $\boldsymbol{q}_g$ where we have to account for fictitious gray walls defined by the new value for A given above, the real value of a has to be taken here.

A word of caution should be added with regard to Traugott's [16] modification if $\alpha_{R_\infty}^*$ differs substantially from $\alpha_{LP_\infty}^*$. In a recent Note [18] Puri and Mandell solved for the flow of a plasma (with $\alpha_{R_\infty}^*/\alpha_{LP_\infty}^* = 1/1936$) past a flat plate by means of the one dimensional "radiation-layer" model. They found that the non-gray exponential-kernel method gives the correct limiting value for $\xi \to 0$ but fails by a large amount for intermediate values of ξ. Since there is a clear connection between the non-gray substitution-kernel method and Traugott's modified differential approximation (see [19]) similar results are obtained with the latter even if the wall radiation is taken into account by Olfe's modification. Therefore it appears that the non-gray differential approximation is not applicable if $\alpha_{R_\infty}^*$ and $\alpha_{LP_\infty}^*$ differ by orders of magnitude.

While Olfe's and Traugott's modification approximately take care of two serious failures of the differential approximation a third complication is the onset of non-linearity if the temperature differences are not small any more. While such a non-linear treatment is outside the scope of this investigation we refer to [20] where the one-dimensional "radiation-layer" problem is solved numerically showing a rather strong dependence on T_P^*/T_∞^*.

CONCLUSION AND EXTENSION

Although the more interesting laterally unbounded case had to be postponed due to the difficult factoring and decomposition in the Wiener–Hopf technique, the laterally bounded problem also gives a clear picture of the influence of convection upon the radiative heat transfer from a hot plate.

As expected the ordinary two-dimensional differential approximation fails near the leading edge of the plate but the error here is much larger than the one usually encountered in one-dimensional gray-gas radiation problems. Assuming that the explicit inclusion of the wall radiation gives us a fairly accurate result we can distinguish three levels of approximation in dealing with the modified differential approximation.

1. Two-dimensional solution with the fully two-dimensional external wall radiation.
2. Two-dimensional solution with a one-dimensional approximation of the external wall radiation.
3. One-dimensional "radiation-layer" solution.

The first two solutions differ only slightly for the range of Bu considered in the present investigation. This surprising fact is of importance because the one-dimensional approximation of the wall radiation amounts to a large simplification in the numerical evaluation of the results as can be seen from the formulas. On the other hand the one-dimensional "radiation-layer" model of Cess appears to be a good approximation only for weak radiation. For intermediate and large values of Γ a distinct precursor effect is observed and, depending on the chosen parameters, the heat flux can deviate considerably from the one-dimensional result.

With regard to the numerical computation it must be said that the given series form of the solution (especially for Θ) is only good for large $|\xi|$ and the convergence is rather slow if $|\xi|$ is small. This situation worsens if Bu and Γ become large. In this case it is advantageous to transform the solution into a form more suitable for numerical computation. For a simpler problem such a procedure has been outlined by Tsien and Finston [21] in the appendix of their paper, but it is not clear how to do this for our problem.

The present work can be extended to include heat conduction if Bo is taken to be zero. In this way the interaction of radiation with heat conduction could be studied for a hot plate. But instead of our simple Wiener–Hopf equation a system of two coupled Wiener–Hopf equations is encountered which, although of a type amenable to solution, is much more difficult to cope with. Last but not least a method similar to Olfe's might prove valuable in investigating the leading edge problem in a rarefied gas if the convective velocities are zero or small.

Acknowledgements—The author wishes to express his sincere gratitude to Dr. W. Schneider for several stimulating and helpful discussions as well as for critically reading the manuscript. The arduous task of programming the results on the CD 6400 has been performed excellently by Mr. L. Leopold whose work is gratefully acknowledged.

REFERENCES

1. R. Viskanta and R. J. Grosh, Boundary layer in thermal radiation absorbing and emitting media, *Int. J. Heat Mass Transfer* **5**, 795–806 (1962).
2. E. M. Sparrow and R. D. Cess, *Radiation Heat Transfer*. Brooks/Cole, Belmont, Ca. (1966).
3. W. G. Vincenti and S. C. Traugott, The coupling of radiative transfer and gas motion, *Annual Review of Fluid Mechanics*, Vol. 3, p. 108. Annual Reviews, Palo Alto, Ca. (1971).
4. D. B. Olfe, A modification of the differential approximation for radiative transfer, *AIAA Jl* **5**, 638–643 (1967).
5. C. S. Landram and R. Greif, Semi-isotropic model for radiation heat transfer, *AIAA Jl* **5**, 1971–1975 (1967).
6. L. R. Glicksman, An approximate method for multi-dimensional problems of radiative energy transfer in an absorbing and emitting media, *J. Heat Transfer* **91C**, 502–510 (1969).
7. S. C. Traugott, An improved differential approximation for radiative transfer with spherical symmetry, *AIAA Jl* **7**, 1825–1832 (1969).
8. I. B. Moreno and I. Greber, New half-range differential approximation for spherically-symmetric radiative transfer, *AIAA Jl* **9**, 2385–2391 (1971).
9. K.-Y. Chien, Application of the S_n method to spherically symmetric radiative-transfer problems, *AIAA Jl* **10**, 55–59 (1972).
10. W. Koch, Application of Olfe's modified differential approximation to the radiation-layer problem on a flat plate, *Int. J. Heat Mass Transfer* **15**, 2663–2667 (1972).
11. W. G. Vincenti and C. H. Kruger, *Introduction to Physical Gas Dynamics*. John Wiley, New York (1965).
12. W. Schneider, Grundlagen der Strahlungsgasdynamik, *Acta Mech.* **5**, 85–117 (1968).
13. B. Noble, *Methods Based on the Wiener–Hopf Technique for the Solution of Partial Differential Equations*. Pergamon Press, Oxford (1958).
14. A. G. Mackie, *Boundary Value Problems*. Oliver & Boyd, London (1965).
15. S. S. Penner and D. B. Olfe, *Radiation and Reentry*, p. 290. Academic Press, New York (1968).
16. S. C. Traugott, Radiative heat-flux potential for a non-gray gas, *AIAA Jl* **4**, 541–542 (1966).
17. A. C. Cogley, W. G. Vincenti and S. E. Gilles, Differential approximation for radiative transfer in a non-grey gas near equilibrium, *AIAA Jl* **6**, 551–553 (1968).
18. R. Puri and D. A. Mandell, Nonviscous nonconducting flow of a radiating plasma over a flat boundary, *J. Heat Transfer* **94C**, 493–494 (1972).
19. S. E. Gilles, A. C. Cogley and W. G. Vincenti, A substitute-kernel approximation for radiative transfer in a nongrey gas near equilibrium, with application to radiative acoustics, *Int. J. Heat Mass Transfer* **12**, 445–458 (1969).

20. Y. Taitel, Exact solution for the "radiation layer" over a flat plate, *J. Heat Transfer* **91C**, 188–189 (1969).
21. H. S. Tsien and M. Finston, Interaction between parallel streams of subsonic and supersonic velocities, *J. Aeronaut. Sci.* **16**, 515–528 (1949).
22. I. S. Gradshteyn and I. M. Ryzhik, *Tables of Integrals, Series and Products.* Academic Press, New York (1965).
23. W. Koch and G. S. S. Ludford, Diffusion in shear flow past a semi-infinite flat plate. Part I. Heat transfer, *Acta Mech.* **10**, 229–250 (1970).
24. D. B. Olfe, Application of a modified differential approximation to radiative transfer in a gray medium between concentric spheres and cylinders, *Jnl Quantve Spectrosc. & Radiat. Transf.* **8**, 899–907 (1968).
25. M. Abramowitz and I. A. Stegun (Editors), *Handbook of Mathematical Functions*, p. 483. Dover, New York (1965).
26. Y. L. Luke, *Integrals of Bessel Functions*, p. 198. McGraw-Hill, New York (1962).
27. Y. L. Luke, *The Special Functions and Their Approximations*, Volume II, p. 342 ff. Academic Press, New York (1969).
28. L. N. G. Filon, On a quadrature formula for trigonometric integrals, *Proc. R. Soc. Edinb.* **49**, 38–47 (1928–29).

APPENDIX A

Solution for the One-Dimensional Model

In order to assess the effects of two-dimensional radiation we need for comparison the solution of the laterally bounded problem according to the one-dimensional model obtained by the same differential approximations. This solution can be found the same way as for the unbounded problem outlined in [10]. To emphasize the common features we formulate the one-dimensional problem also in terms of I_g and use the one-sided Fourier transformation instead of the more common Laplace transformation.

Thus, assuming that changes in the transverse radiative transfer predominate over that in flow direction our basic equation (5) reduces to

$$\frac{Bo}{3Bu^2}\frac{\partial^2}{\partial y^2}\left(\frac{\partial \hat{I}_g}{\partial x}+\frac{16Bu}{Bo}\hat{I}_g\right)-Bo\frac{\partial \hat{I}_g}{\partial x}=\hat{Q}(y), \tag{A.1}$$

where now (see for example [4] and [10])

$$\hat{q}_{\text{ext}}(y)=2E_3(Bu\,.\,y) \tag{A.2}$$

and hence

$$\hat{Q}(y)\equiv 4\frac{\mathrm{d}\hat{q}_{\text{ext}}}{\mathrm{d}y}=-8BuE_2(Bu\,.\,y). \tag{A.3}$$

In the one-dimensional problem disturbances are limited to the region $x \geqslant 0$ so that we also need to specify the "initial condition"

$$\hat{I}_g(0,y)=0. \tag{A.4}$$

(a) *Solution according to the ordinary differential approximation*

With $\hat{Q}\equiv 0$ we take the one-sided Fourier transform, defined by

$$\bar{f}(\lambda)=\int_0^\infty \mathrm{e}^{-i\lambda x}f(x)\,\mathrm{d}x,\quad Im\lambda<0,$$

of the homogeneous equation (A.1) and the boundary conditions (7) and (8a), with due consideration of (A.4), and solve the ordinary differential problem for $\bar{\hat{I}}_g(y;\lambda)$. Again we are mostly interested in the heat transfer and gas temperature on the plate. The latter can be found from $\bar{\hat{I}}_g$ by means of the transformed equations (1) and (3). Thus, in the complex plane

$$\bar{\hat{q}}_y(0;\lambda)=-\frac{4i}{3Bu\lambda}\frac{\cosh\hat{m}+\dfrac{2\hat{m}}{3Bu}\sinh\hat{m}}{\dfrac{4}{3Bu}\cosh\hat{m}+\dfrac{\sinh\hat{m}}{\hat{m}}\left[1+\left(\dfrac{2\hat{m}}{3Bu}\right)^2\right]}, \tag{A.5}$$

$$\bar{\hat{\Theta}}(0;\lambda)=-\frac{16}{3Bo}\frac{2}{\lambda(\lambda-i16Bu/Bo)}\times\frac{\cosh\hat{m}+\dfrac{3Bu}{2\hat{m}}\sinh\hat{m}}{\dfrac{4}{3Bu}\cosh\hat{m}+\dfrac{\sinh\hat{m}}{\hat{m}}\left[1+\left(\dfrac{2\hat{m}}{3Bu}\right)^2\right]}, \tag{A.6}$$

with

$$\hat{m}=Bu\{3\lambda/(\lambda-i16Bu/Bo)\}^{1/2}.$$

As for the two-dimensional problem we can easily show that both $\bar{\hat{q}}_y(0;\lambda)$ and $\bar{\hat{\Theta}}(0;\lambda)$ are single-valued functions of λ. Instead of the finite branch cut in the laterally unbounded problem, discussed in [10], our functions now exhibit an infinite number of poles at

$$\lambda=0\quad\text{and}\quad\lambda=i\hat{\tau}_k,\quad \hat{\tau}_k=\frac{16Bu}{Bo}\frac{\beta_k^2}{3Bu^2+\beta_k^2},\quad k=1,2,\ldots,$$

with an accumulation point at $\lambda=i16Bu/Bo$. Since the main part of the denominator of the above functions (A.5), (A.6) and of $K(\hat{m})$, as given by (15), coincide in the m-plane, the β_k's are those defined in Appendix B. Now the inversion of (A.5) and (A.6) by means of the residue theorem gives in terms of our "radiation-layer" variable ξ

$$\hat{q}_y(\xi,0^+)=\frac{1}{1+3Bu/4}+6Bu^2\sum_{n=1}^{\infty}\frac{1}{3Bu^2+\beta_n^2}\times\frac{\exp[-8\beta_n^2\xi/(3Bu^2+\beta_n^2)]}{1+\dfrac{3Bu}{4}\left[1+\left(\dfrac{2\beta_n}{3Bu}\right)^2\right]}, \tag{A.7}$$

$$\hat{\Theta}(\xi,0)=\frac{1+3Bu/2}{2+3Bu/2}-\sum_{n=1}^{\infty}\times\frac{\exp[-8\beta_n^2\xi/(3Bu^2+\beta_n^2)]}{1+3Bu[1+\{2\beta_n/(3Bu)\}^2]/4}. \tag{A.8}$$

Figure 5 shows $\hat{q}_y(\xi,0)$ for several values of Bu.

(b) *Solution according to Olfe's modified differential approximation*

Now we take the one-sided Fourier transform of the inhomogeneous equation (A.1) as well as of the homogeneous boundary conditions (7) and (8b). A particular solution of the corresponding ordinary, inhomogeneous differential

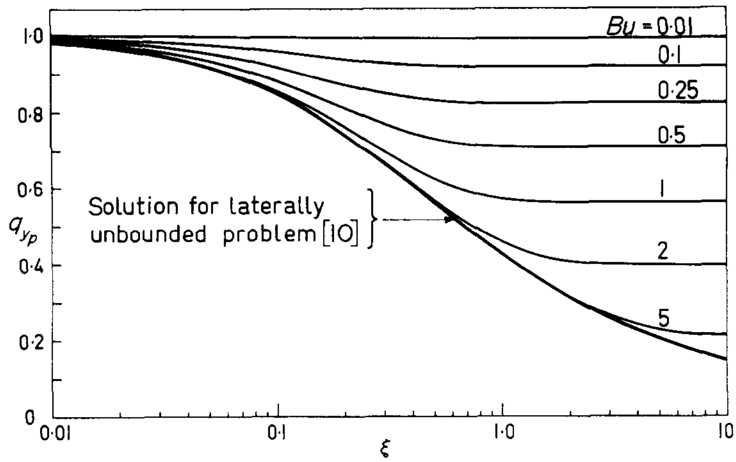

FIG. 6. One-dimensional solution for the non-dimensional linearized radiative heat flux normal to the black-body plate as a function of ξ and Bu according to Olfe's modified differential approximation.

equation is easily found by the method of variation of parameters, so that for $y = 0$

$$\bar{q}_{y_g}(0;\lambda) = \frac{4}{3}\frac{16Bu/Bo}{\lambda(\lambda - i16Bu/Bo)} \times \frac{\int_0^1 \left\{\cosh[\hat{m}(1-\eta)] + \frac{3Bu}{2\hat{m}}\sinh[\hat{m}(1-\eta)]\right\}E_2(Bu\eta)\,d\eta}{\frac{4}{3Bu}\cosh\hat{m} + \frac{\sinh\hat{m}}{\hat{m}}[1+\{2\hat{m}/(3Bu)\}^2]},$$

$$\bar{\Theta}(0;\lambda) = i\frac{2}{3}\frac{(16Bu/Bo)^2}{\lambda(\lambda - i16Bu/Bo)^2} \times \frac{\int_0^1 \left\{\cosh[\hat{m}(1-\eta)] + \frac{3Bu}{2\hat{m}}\sinh[\hat{m}(1-\eta)]\right\}E_2(Bu\eta)\,d\eta}{\frac{4}{3Bu}\cosh\hat{m} + \frac{\sinh\hat{m}}{\hat{m}}[1+\{2\hat{m}/(3Bu)\}^2]} - \frac{8Bu/Bo}{\lambda(\lambda - i16Bu/Bo)}.$$

Observing that $\hat{q} = \hat{q}_g + \hat{q}_{ext}$ we obtain the final results by inversion of the above equations together with (A.2)

$$\hat{q}(\xi, 0^+) = \frac{1}{1+3Bu/4}\{1 + E_3(Bu) - 3E_4(Bu)/2\} + 2Bu\sum_{n=1}^{\infty}\frac{\mathscr{B}_n^{(0)}\exp[-8\beta_n^2\xi/(3Bu^2+\beta_n^2)]}{1+3Bu[1+\{2\beta_n/(3Bu)\}^2]/4},$$

$$\hat{\Theta}(\xi, 0) = \frac{1}{2+3Bu/2}\{1 + 3Bu/2 - E_3(Bu) + 3E_4(Bu)/2\} - \frac{1}{3Bu}\sum_{n=1}^{\infty}\frac{\mathscr{B}_n^{(0)}(3Bu^2+\beta_n^2)\exp[-8\beta_n^2\xi/(3Bu^2+\beta_n^2)]}{1+3Bu[1+\{2\beta_n/(3Bu)\}^2]/4}.$$

$\mathscr{B}_n^{(0)}$ can be evaluated explicitly by using relation 5.231 (2) on page 632 of [22] so that after integrating by parts once:

$$\begin{aligned}\mathscr{B}_n^{(0)} &\equiv \int_0^1 \left\{\cos(\beta_n\eta) + \frac{3Bu}{2\beta_n}\sin(\beta_n\eta)\right\}E_2(Bu\eta)\,d\eta \\ &= \frac{Bu}{\beta_n^2}(3/2 - \log Bu) + \left\{\frac{\sin\beta_n}{\beta_n} - \frac{3Bu}{2\beta_n^2}\cos\beta_n\right\}E_2(Bu) \\ &\quad - \frac{Bu}{\beta_n^2}\left\{\cos\beta_n + \frac{3Bu}{2\beta_n}\sin\beta_n\right\}E_1(Bu) \\ &\quad + \frac{Bu}{\beta_n^2}\left\{Re[E_1(Bu+i\beta_n) + \log(Bu+i\beta_n)]\right. \\ &\quad \left. - \frac{3Bu}{2\beta_n}Im[E_1(Bu+i\beta_n) + \log(Bu+i\beta_n)]\right\}. \end{aligned} \quad \text{(A.9)}$$

The results for $\hat{q}(\xi, 0)$ and $\hat{\Theta}(\xi, 0)$ according to Olfe's modified differential approximation are shown in Figs. 6 and 7 for several values of Bu. The laterally unbounded solution [10] is approached as Bu becomes large, since then the influence of the side walls is small. The failure of the ordinary differential approximation near the leading edge of the plate shows up clearly but is less pronounced compared to the two-dimensional case.

APPENDIX B

Zeros and Poles of $K(\lambda)$

To compute the zeros and poles of $K(\lambda)$ it is of advantage to first locate the zeros and poles of K in the m-plane*. Both, numerator and denominator of K are even functions of m and hence their roots occur in pairs. Furthermore

*The author is grateful to Dr. Anneliese Frohn for this suggestion.

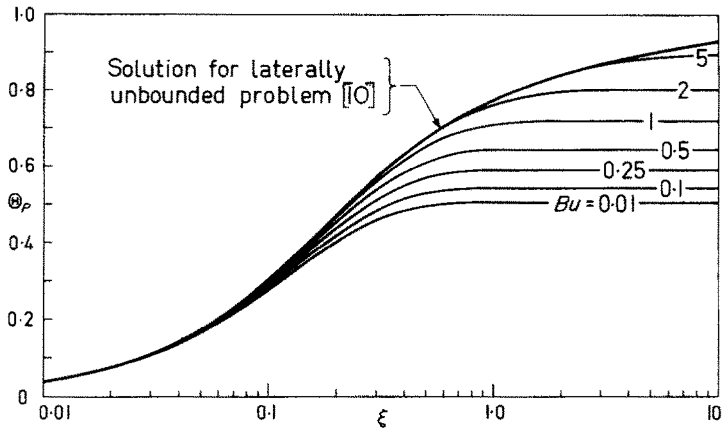

FIG. 7. One-dimensional solution for the non-dimensional gas temperature on the black-body plate as a function of ξ and Bu according to Olfe's modified differential approximation.

these roots are purely imaginary so that by means of the infinite-product theorem

$$K(m) = -\frac{3Bu/2}{2+3Bu/2}\prod_{k=1}^{\infty}\frac{1+(m/\gamma_k)^2}{1+(m/\beta_k)^2}. \quad \text{(B.1)}$$

The roots $m = \pm i\gamma_k$ and $m = \pm i\beta_k$, $k = 1,2,\ldots$, are only functions of Bu and their numerical values can easily be computed for example by means of Newton's method. For large k

$$\gamma_k \sim k\pi\left\{1+\frac{3Bu/2}{k^2\pi^2}+\ldots\right\},$$

$$\beta_k \sim k\pi\left\{1+\frac{3Bu}{k^2\pi^2}+\ldots\right\},$$

so that obviously no convergence factor is needed in (B.1). For the special case of zero convection, i.e. $Bo = 0$, the governing equation (5) reduces to Poisson's equation and (9) simplifies to $m = \lambda$. Hence for radiative heat transfer without convection (B.1) is already the infinite product representation of $K(\lambda)$.

If $Bo \neq 0$ and with m given by (9) we have to solve, for a given k, a complex algebraic equation of third degree in order to obtain the zeros and poles of K in the λ-plane. In other words each γ_k^2 or β_k^2, $k = 1,2,\ldots$, generates three zeros or poles of K respectively. Drawing on the corresponding one-dimensional result given in Appendix A and some experience gained in treating a related heat-conduction problem [23] we make the *ad hoc* assumption that all zeros and poles of K are purely imaginary. This simplifies our problem because now we only have to solve a real algebraic equation of third degree which can be done by standard methods. We introduce the abbreviations

$$\left.\begin{aligned} b(\beta_k^2) &= 1+\frac{Bu^2+\beta_k^2/3}{\Gamma^2(1+Bu^2)^2} \\ c(\beta_k^2) &= -\left[1+\frac{3Bu^2/2-\beta_k^2}{\Gamma^2(1+Bu^2)^2}\right] \end{aligned}\right\} \quad k = 1,2,\ldots.$$

Then by expressing all terms as positive squares we can show that

$$b^3(\beta_k^2)-c^2(\beta_k^2) > 0, \quad k = 1,2,\ldots,$$

and hence all poles of K actually lie on the imaginary axis as has been assumed. Furthermore, for each k always one pole lies on the negative imaginary axis while the remaining two are positive imaginary. As $k \to \infty$ one of the latter (namely $i\tau_k^{(1)}$) has an accumulation point at $\lambda = i16Bu/Bo$ and hence can be considered a modification of the pole $\hat{\tau}_k$ of the one-dimensional problem treated in Appendix A. The other two, with accumulation points at infinity, are new and are the mathematical consequence of our two-dimensional treatment. If we substitute γ_k^2 for β_k^2 in the above formulas, similar results can be proved for all zeros of $K(\lambda)$. Thus, with

$$\Psi(\beta_k^2) = \arccos[-c(\beta_k^2)/b^{3/2}(\beta_k^2)], \quad k = 1,2,\ldots,$$

$K(\lambda)$ has poles at

$$\begin{aligned}\lambda = -i\sigma_k &\equiv -i2\frac{Bu}{Bo}\tilde{\sigma}_k(Bu,\Gamma) \\ &= i\frac{16Bu}{3Bo}\{1+2[b(\beta_k^2)]^{1/2}\cos[(\Psi(\beta_k^2)+2\pi)/3]\},\end{aligned}$$

$$\begin{aligned}\lambda = i\tau_k^{(1)} &\equiv i2\frac{Bu}{Bo}\tilde{\tau}_k^{(1)}(Bu,\Gamma) \\ &= i\frac{16Bu}{3Bo}\{1+2[b(\beta_k^2)]^{1/2}\cos[(\Psi(\beta_k^2)+4\pi)/3]\},\end{aligned}$$

$$\begin{aligned}\lambda = i\tau_k^{(2)} &\equiv i2\frac{Bu}{Bo}\tilde{\tau}_k^{(2)}(Bu,\Gamma) \\ &= i\frac{16Bu}{3Bo}\{1+2[b(\beta_k^2)]^{1/2}\cos[\Psi(\beta_k^2)/3]\},\end{aligned}$$

$$k = 1,2,\ldots.$$

Correspondingly we find $K(\lambda)$ has zeros at

$$\lambda = -i\mu_k \equiv -i2\frac{Bu}{Bo}\tilde{\mu}_k(Bu,\Gamma)$$
$$= i\frac{16Bu}{3Bo}\{1+2[b(\gamma_k^2)]\cos[(\Psi(\gamma_k^2)+2\pi)/3]\},$$

$$\lambda = i\nu_k^{(1)} \equiv i2\frac{Bu}{Bo}\tilde{\nu}_k^{(1)}(Bu,\Gamma)$$
$$= i\frac{16Bu}{3Bo}\{1+2[b(\gamma_k^2)]\cos[(\Psi(\gamma_k^2)+4\pi)/3]\},$$

$$\lambda = i\nu_k^{(2)} \equiv i2\frac{Bu}{Bo}\tilde{\nu}_k^{(2)}(Bu,\Gamma)$$
$$= i\frac{16Bu}{3Bo}\{1+2[b(\gamma_k^2)]\cos[\Psi(\gamma_k^2)/3]\},$$
$$k = 1, 2, \ldots.$$

With these results the infinite product representation (16), (17) follows at once. Again no convergence factor is needed.

APPENDIX C

Evaluation of the External Heat-Source Distribution Q(x, y)

To obtain the heat-source distribution $Q(x,y)$, which according to our defining equations (1), (2) and (5) equals

$$Q(x,y) = 4\,\mathrm{div}\,\boldsymbol{q}_{\mathrm{ext}}, \qquad \text{(C.1)}$$

we need to compute the non-dimensional net flux $\boldsymbol{q}_{\mathrm{ext}}$ due to black-body radiation from a semi-infinite plate at temperature T_P^* and two enclosing parallel walls at temperature $T_\infty^* < T_P^*$ (see Fig. 1). For this calculation the medium is assumed to only absorb but not to emit radiation. Hence, omitting the emission term, simple integration of the equation of radiative transfer along the propagation direction s (with unit vector $\boldsymbol{l}$) gives the perturbation quantity

$$I_{\mathrm{ext}}(s,\boldsymbol{l}) = \exp(-Bus).$$

From this the non-dimensional net flux $\boldsymbol{q}_{\mathrm{ext}}$ is computed by integrating the components of I_{ext} over the solid angle

$$\boldsymbol{q}_{\mathrm{ext}} = \frac{1}{\pi}\int_0^{4\pi} \boldsymbol{l} I_{\mathrm{ext}}(s,\boldsymbol{l})\,\mathrm{d}\Omega.$$

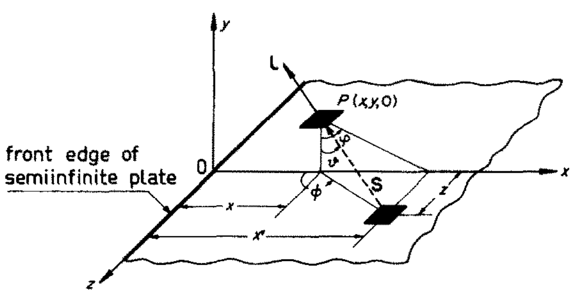

FIG. 8. Geometry for the computation of $\boldsymbol{q}_{\mathrm{ext}}$.

In analogy to the coordinate system employed by Olfe for the cylindrical problem [24] we use the one shown in Fig. 8 and find

$$\boldsymbol{q}(x,y)_{\mathrm{ext}} \equiv \begin{Bmatrix}(q_{\mathrm{ext}})_x\\ (q_{\mathrm{ext}})_y\end{Bmatrix}$$
$$= \frac{2}{\pi}\int_{x'=0}^{\infty}\int_{z=0}^{\infty}\begin{Bmatrix}\sin\vartheta\cos\phi\\ \cos\vartheta\end{Bmatrix}e^{-Bus}\frac{\cos\vartheta}{s^2}\,\mathrm{d}x'\,\mathrm{d}z,$$
$$s = \{(x-x')^2+y^2+z^2\}^{1/2}.$$

Changing variables according to

$$z = \{(x-x')^2+y^2\}^{1/2}\sinh t,$$
$$\varphi = \arctan\{(x'-x)/y\}$$

$\boldsymbol{q}_{\mathrm{ext}}$ can be expressed in the form

$$\boldsymbol{q}(x,y)_{\mathrm{ext}} = \frac{2}{\pi}\int_{\varphi=-\arctan(x/y)}^{\pi/2} \times\begin{Bmatrix}-\sin\varphi\\ \cos\varphi\end{Bmatrix} Ki_3(Buy/\cos\varphi)\,\mathrm{d}\varphi. \qquad \text{(C.2)}$$

Here

$$Ki_n(z) \equiv \int_0^{\infty}\frac{\exp(-z\cosh t)}{\cosh^n t}\,\mathrm{d}t, \qquad \text{(C.3)}$$

as defined in [25], is the nth repeated integral of the modified Bessel function $K_0(z)$ and is a special case of the function

$$K_{\alpha,\nu}(z) = \int_0^{z}\exp(-z\cosh t)\frac{\cosh \nu t}{\cosh^{\alpha} t}\,\mathrm{d}t$$

discussed for example in [26]. Now with (C.1) and (C.3) we immediately find from (C.2)

$$Q(x,y) = -\frac{8Bu}{\pi}\int_{\varphi=-\arctan(x/y)}^{\pi/2} Ki_2(Buy/\cos\varphi)\,\mathrm{d}\varphi. \qquad \text{(C.4)}$$

The function $Ki_2(z)$ can be evaluated numerically by means of the recurrence relation (cf. [25]) using Chebyshev approximations for

$$Ki_1(z) = \int_z^{\infty} K_0(t)\,\mathrm{d}t$$

as given for example in [27]. While the external source distribution in the cylindrical problem [24] only depends on the radius, we have a truely two-dimensional dependence in our case. To obtain an idea about the magnitude of $Q(x,y)$ the source distribution is shown in Fig. 9 for two values of Bu [$Q(x,y)$ does not depend on Γ].

As $x \to \infty$ the one-dimensional problem, discussed in Appendix A, is approached and by comparing the corresponding quantities for $\boldsymbol{q}_{\mathrm{ext}}$ and $Q(x,y)$ we can derive the useful relations

$$\frac{1}{\pi}\int_{\varphi=-\pi/2}^{\pi/2}\cos\varphi\, Ki_3(Buy/\cos\varphi)\,\mathrm{d}\varphi = E_3(Buy),$$
$$\frac{1}{\pi}\int_{\varphi=-\pi/2}^{\pi/2} Ki_2(Buy/\cos\varphi)\,\mathrm{d}\varphi = E_2(Buy).$$

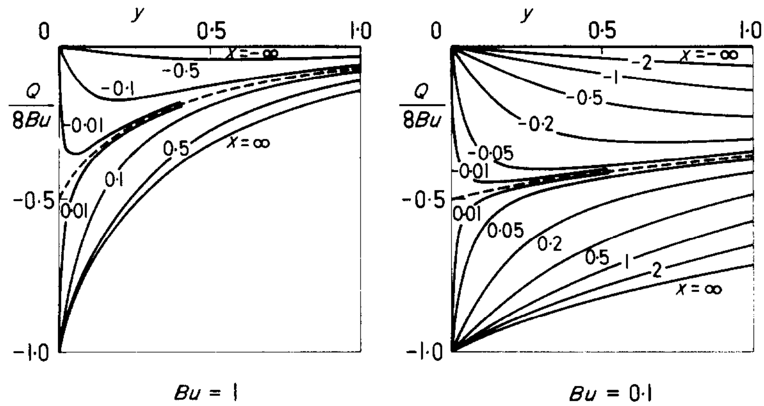

FIG. 9. Two-dimensional source function due to plate emission for $Bu = 1$ and $Bu = 0{\cdot}1$.

APPENDIX D

Additive Decomposition of $D(\lambda)$

For the additive decomposition of $D(\lambda)$ and in order to clearly demonstrate the influence of the two-dimensional source distribution it is advantageous to write

$$Q(x, y) = \hat{Q}(y) + Q'(x, y).$$

Here $\hat{Q}(y)$ is the source distribution (A.3) according to the one-dimensional model while $Q'(x, y)$ denotes the two-dimensional correction. Using (C.4) it is easily checked that $Q'(x, y)$ is an odd function of x with

$$Q'(x, y) = \frac{8\,Bu}{\pi}\int_{\arctan(x/y)}^{\pi/2} Ki_2(Buy/\cos\varphi)\,\mathrm{d}\varphi, \quad x > 0.$$

Unfortunately, it appears to be impossible to obtain an explicit Fourier transform of $Q'(x, y)$ in terms of known functions. So, making use of $Q'(x, y)$ being an odd function of x, we help ourselves by writing

$$\bar{Q}(y;\lambda) = \left[\frac{\hat{Q}(y)}{i\lambda}\right]_{\ominus} - \left[\int_0^\infty Q'(x, y)\,\mathrm{e}^{i\lambda x}\,\mathrm{d}x\right]_{\oplus} + \left[\int_0^\infty Q'(x, y)\,\mathrm{e}^{-i\lambda x}\,\mathrm{d}x\right]_{\ominus}. \quad \text{(D.1)}$$

Substituting this into (24) we get correspondingly $D(\lambda)$ as the sum of three parts, i.e.

$$D(\lambda) = \hat{D}(\lambda) - D(\lambda)^{(+)} + D(\lambda)^{(-)}.$$

Now each of these three functions has to be decomposed into two parts, regular in an upper and lower half plane respectively. A straight forward application of the formal decomposition theorem (cf. [13], p. 13) gives, after a rather tedious evaluation of the integrals by means of the residue theorem, first for $\hat{D}(\lambda)$:

$$\hat{D}(\lambda)_{\oplus} = -i\frac{16\,Bu^2}{Bo}K(0)\sum_{m=1}^{\infty}\frac{S_m\mathscr{B}_m^{(0)}}{(\sigma_m + 16\,Bu/Bo)(\lambda + i\sigma_m)},$$

$$\hat{D}(\lambda)_{\ominus} = -i\frac{K(0)}{\lambda}\{3\,Bu/4 - E_3(Bu) + 3\,E_4(Bu)/2\} + i\frac{24\,Bu^3}{Bo}\sum_{j=1}^{2}\sum_{m=1}^{\infty}\frac{N_{m,j}\mathscr{A}_m^{(0)}}{(v_m^{(j)} - 16\,Bu/Bo)(\lambda - iv_m^{(j)})}.$$

$K(0)$ is simply

$$\left\{-\frac{3\,Bu/2}{2 + 3\,Bu/2}\right\}$$

from (17a), $\mathscr{B}_m^{(0)}$ is evaluated in Appendix A, equation (A.9), while a similar integration gives

$$\mathscr{A}_m^{(0)} \equiv \int_0^1 \cos(\gamma_m\eta)E_2(Bu\eta)\,\mathrm{d}\eta = \sin\gamma_m E_2(Bu)/\gamma_m - \frac{Bu}{\gamma_m^2}\{E_1(Bu)\cos\gamma_m + \log Bu - Re[E_1(Bu + i\gamma_m) + \log(Bu + i\gamma_m)]\}. \quad \text{(D.2)}$$

The coefficients S_m and $N_{m,j}$ are defined by

$$S_m = (1 - \sigma_m/\mu_m)\prod_{k(\neq m)=1}^{\infty}\frac{(1 - \sigma_m/\mu_k)}{(1 - \sigma_m/\sigma_k)}, \quad \text{(D.3)}$$

$$N_{m,1} = \frac{(1 - v_m^{(1)}/\tau_m^{(1)})(1 - v_m^{(1)}/\tau_m^{(2)})}{(1 - v_m^{(1)}/v_m^{(2)})} \times \prod_{k(\neq m)=1}^{\infty}\frac{(1 - v_m^{(1)}/\tau_k^{(1)})(1 - v_m^{(1)}/\tau_k^{(2)})}{(1 - v_m^{(1)}/v_k^{(1)})(1 - v_m^{(1)}/v_k^{(2)})}, \quad \text{(D.4a)}$$

$$N_{m,2} = \frac{(1 - v_m^{(2)}/\tau_m^{(1)})(1 - v_m^{(2)}/\tau_m^{(2)})}{(1 - v_m^{(2)}/v_m^{(1)})} \times \prod_{k(\neq m)=1}^{\infty}\frac{(1 - v_m^{(2)}/\tau_k^{(1)})(1 - v_m^{(2)}/\tau_k^{(2)})}{(1 - v_m^{(2)}/v_k^{(1)})(1 - v_m^{(2)}/v_k^{(2)})}. \quad \text{(D.4b)}$$

Making use of the region of regularity for the second and third part on the r.h.s. of (D.1) we obtain by an equivalent procedure

$$D(\lambda)_{\oplus}^{(-)} = i\frac{2\,Bu}{Bo}K(0)\sum_{m=1}^{\infty}\frac{\sigma_m S_m\mathscr{B}_m^{(1)}}{(\sigma_m + 16\,Bu/Bo)(\lambda + i\sigma_m)},$$

$$D(\lambda)_{\ominus}^{(+)} = i\frac{3\,Bu^2}{Bo}\sum_{j=1}^{2}\sum_{m=1}^{\infty}\frac{v_m^{(j)}N_{m,j}\mathscr{A}_{m,j}^{(1)}}{(v_m^{(j)} - 16\,Bu/Bo)(\lambda - iv_m^{(j)})}.$$

The remaining two functions $D(\lambda)_{\ominus}^{(-)}$ and $D(\lambda)_{\oplus}^{(+)}$ are recovered by simple subtraction

$$D(\lambda)_{\ominus}^{(-)} = D(\lambda)^{(-)} - D(\lambda)_{\oplus}^{(-)},$$

$$D(\lambda)_{\oplus}^{(+)} = D(\lambda)^{(+)} - D(\lambda)_{\ominus}^{(+)}.$$

For the coefficients $\mathscr{A}^{(1)}_{m,j}$ and $\mathscr{B}^{(1)}_m$ we have the definitions

$$\mathscr{A}^{(1)}_{m,j} = \int_{\eta=0}^{1} \cos(\gamma_m \eta) \int_{\zeta=0}^{\infty} Q'(\zeta,\eta) \exp\{-\nu^{(j)}_m \zeta\} \, d\zeta \, d\eta, \quad (D.5)$$

$$\mathscr{B}^{(1)}_m = \int_{\eta=0}^{1} \left\{ \cos(\beta_m \eta) + \frac{3Bu}{2\beta_m} \sin(\beta_m \eta) \right\} \int_{\zeta=0}^{\infty} Q'(\zeta,\eta) \exp\{-\sigma_m \zeta\} \, d\zeta \, d\eta \quad (D.6)$$

Contrary to $\mathscr{A}^{(0)}_m$ and $\mathscr{B}^{(0)}_m$ the above integrals as well as those for $\mathscr{C}_n$ and $\mathscr{D}_n$ defined by (28) and (29) respectively have to be computed numerically. For the η-integration we used Filon's classical quadrature formula [28] with 50 intervals. The ζ-integration was performed by using a Gauss quadrature formula of order 10 whereby the upper limit has been chosen arbitrarily at such a location where $Q'(\zeta,\eta)$ was less than 10^{-6}.

INTERACTION RAYONNEMENT–CONVECTION POUR UN ECOULEMENT LIMITE PAR UNE PLAQUE CHAUDE

Résumé—On étudie l'intéraction rayonnement–convection pour un écoulement limité latéralement par une plaque chauffée, en s'intéressant à l'influence du rayonnement bidimensionnel. A cause de la grande anisotropie du rayonnement près du bord d'attaque de la plaque, l'approximation bidimensionnelle aux dérivées partielles tombe en défaut dans cette région. On utilise l'approximation de Olfe qui tient compte séparément du rayonnement externe de la paroi. Ces équations pour un gaz gris sont linéarisées en admettant de faibles perturbations de température et elles sont résolues par la technique Wiener–Hopf. On compare les résultats avec des solutions approchées. En particulier on montre que le modèle monodimensionnel de "couche de rayonnement" de Cess est limité au rayonnement faible. On constate un comportement différant pour un rayonnement intermédiaire ou fort.

WECHSELWIRKUNG ZWISCHEN STRAHLUNG UND KONVEKTION BEI EINER SEITLICH BEGRENZTEN STRÖMUNG UM EINE BEHEIZTE PLATTE

Zusammenfassung—Die Wechselwirkung zwischen Strahlung und Konvektion in einer seitlich begrenzten Strömung um eine beheizte Platte wird untersucht, wobei der Einfluß zweidimensionaler Strahlung im Vordergrund steht. Wegen der starken Anisotropie der Strahlung nahe der Plattenvorderkante versagt die gewöhnliche, zweidimensionale Differentialapproximation in diesem Gebiet. Es wird deshalb eine nach Olfe modifizierte Differentialapproximation verwendet, bei welcher die Wandstrahlung gesondert berücksichtigt wird. Die Gleichungen für ein graues Gas werden unter der Annahme kleiner Temperaturströrungen linearisiert und mittels der Wiener-Hopf-Methode gelöst. Die Resultate werden mit verschiedenen Näherungslösungen verglichen. Dabei zeigt sich unter anderem, daß der Anwendungsbereich des eindimensionalen "Strahlungsschichtmodells" von Cess auf schwache Strahlung beschränkt ist. Für mittlere und starke Strahlung wird ein ausgeprägter "Vorläufereffekt" beobachtet.

ВЛИЯНИЕ ИЗЛУЧЕНИЯ И КОНВЕКЦИИ ПРИ ОБТЕКАНИИ НАГРЕТОЙ ПЛАСТИНЫ ПОТОКОМ, ОГРАНИЧЕННЫМ БОКОВЫМИ СТЕНКАМИ

Аннотация — Проведено исследование влияния излучения и конвекции при обтекании нагретой пластины потоком, ограниченным боковыми стенками, причём влияние двумерного излучения является преобладающим. Вследствие высокой анизотропии излучения вблизи передней кромки пластины обычное двумерное приближение оказывается недостаточным. Поэтому используется модифицированное дифференциальное приближение Ольфе, в котором учитывается излучение внешней стенки. Уравнения для серого газа линеаризуются в предположении малых температурных возмущений и решаются методом Винера–Хопфа. Результаты исследования сравниваются с некоторыми приближенными решениями. Показано также, что одномерная модель «слоя излучения» Сесса ограничивается областью малой интенсивности излучения. Для излучения средней и большой инт нсивности наблюда тся ярко выраж нно влияние предыстории потока.